PNAS
www.pnas.org

Supplementary Information for

# Intracellular $Ca^{2+}$ regulation of $H^+/Ca^{2+}$ antiporter YfkE mediated by a $Ca^{2+}$ mini-sensor

Shuo Lu, Zhenlong Li, Alemayehu A. Gorfe and Lei Zheng

Corresponding author: Lei Zheng
Email: lei.zheng@uth.tmc.edu

**This PDF file includes:**

Supplementary text
Figures S1 to S9
Legends for Movies S1 to S2
SI References

**Other supplementary materials for this manuscript include the following:**

Movies S1 to S2

## Supplementary text

***Full details of Materials and Methods***

**Preparation of inside-out vesicles**— Inside-out (ISO) vesicles were prepared using low-pressure homogenization as described in our previous study (1). Briefly, *E. coli* BL21(DE3) cells harboring a pET28a-YfkE vector were grown in Luria broth medium at 37°C to $A_{600}$ of 0.4. Protein expression was induced by adding 0.2 mM isopropyl β-D-1-thiogalactopyranoside (IPTG) for 2 h at 25°C. Cells were washed with buffer containing 10 mM Tris-HCl pH 7.3, 140 mM KCl, 0.5 mM DTT, 250 mM sucrose. Cell rupture was processed by single passage through a C3 homogenizer (Avestin) with a low pressure (4,000 *p.s.i.*). After removing cell debris by centrifugation, supernatants were centrifuged using a Ti45 rotor at 40,000 rpm for 1 h to pellet membrane vesicles. Vesicles were homogenized in the same buffer and then quickly frozen in liquid Nitrogen prior to use. Mutations were generated using a standard Quick-Change site-directed mutagenesis approach and confirmed by sequencing.

**$Ca^{2+}$ transport assay**— The $Ca^{2+}$ efflux activity of YfkE was determined by measuring $^{45}Ca^{2+}$ influx into ISO vesicles as we described previously (1). Briefly, ISO vesicles were diluted in buffer (pH 8.0) to a total protein concentration of 0.13 mg/ml. Prior to assays, 5 mM NADH and 5 mM potassium phosphate were added to the solution for 10 min to establish an outward $H^+$ gradient. Free $Ca^{2+}$ concentrations were determined using Ca-EGTA calculator v.1.3 ( https://somapp.ucdmc.ucdavis.edu/pharmacology/bers/maxchelator/CaEGTA-TS.htm) by titrating $Ca^{2+}$ into 1 mM EGTA. $Ca^{2+}$ influx was triggered by adding $^{45}CaCl_2$ (Perkin Elmer) into the reactions at room temperature. Reactions were stopped by filtration through a nitrocellulose membrane (0.22 μm) on a Millipore filtration manifold and washed immediately with 10 ml buffer. The filters were air-dried and counted in a liquid scintillation counter to determine transport activity. For kinetic analysis, data fitting was performed using the software Graphpad Prism 7 to calculate kinetic constants. ISO vesicles prepared with *E. coli* cells harboring empty vector were used as control. For peptide inhibition assays, custom synthesized peptides of XIP and variant (95% purity, Biomatik) were dissolved in vesicle buffer and incubated with the vesicles for 10 min on ice prior to transport assays. Chemical modification of the peptide was performed using phenylglyoxal by following a published protocol (2). Specifically, 50μM peptide was incubated with 5 mM phenylglyoxal at room temperature for 2 h. The reaction was quenched by adding 10 mM free arginine and diluted at least 10x prior to use.

**Protein expression and purification**— The proteins of YfkE wild type and variants were expressed and purified as described in our previous structural study (1). Briefly, protein expression was carried out in *E. coli* C41(DE3) strain in auto-induction medium (3) at 25 ºC overnight. Cells were suspended in a buffer containing 20 mM sodium phosphate, pH 7.4, 500 mM NaCl and 20 mM imidazole and then ruptured by three passages through a C3 homogenizer (Avestin) at 15,000 *p.s.i.* Membrane fractions were collected as described above and suspended in lysis buffer. Membrane fractions were solubilized by adding 1% (w/v) n-dodecyl-β-maltoside (DDM) at 4 °C for 1 h and incubated with Ni-NTA resin (GE healthcare). Resins were washed with buffer supplemented with 60 mM imidazole and 0.05% DDM, and then eluted with buffer supplemented with 400 mM imidazole and 0.05% DDM. The eluted protein was further purified using a Superdex-200 10/300 GL column (GE Healthcare) equilibrated in a buffer containing 20 mM HEPES (pH 7.4), 500 mM NaCl and 0.05% DDM.

**Isothermal titration calorimetry**— $Ca^{2+}$ binding affinity was determined using isothermal titration calorimetry (ITC) by following a procedure we previously described (4). The YfkE proteins were first decalcified by adding 10 mM EGTA, and then separated using size-exclusion chromatography. The $Ca^{2+}$ solution was prepared in the same buffer. ITC assays were performed by titrating $Ca^{2+}$ into a solution of 5 μM YfkE protein on a VP-ITC device (MicroCal). All assays used the same ITC procedure: The system was thermally equilibrated at 25 °C; after an initial delay of 120 s, serial injections (10 μl each) were done with a spacing time of 240 s at 307 rpm stirring speed. Each measurement was corrected with a background titration in which the ligand was titrated into a buffer solution. Data fitting was carried out using the software Origin (Microcal LLC). A synthetic peptide representing the TM5-6 loop of YfkE was dissolved in a buffer of 20 mM Tris-HCl, 50 mM NaCl, pH 8. 10 μM peptide was titrated with a solution of 2 mM cation. ITC measurements with $Mg^{2+}$, $Cd^{2+}$, $K^+$, and $Na^+$ were measured on a nanoITC device (Malvern MicroCAL). The data were processed using the software nanoAnalyze.

**Fluorescence resonance energy transfer (FRET)**— Protein conformational changes were monitored using FRET by labelling the YfkE$^{A190C}$ mutant protein with a pair of fluorescence dyes, Alexa Fluor 555 and 647. Specifically, 5 μM proteins were mixed with Alexa Fluor 555 maleimide and Alex Fluor 647 maleimide (Life Technologies, CA) in a 1:1:2 molar ratio at 4°C overnight. The reactions were separated using a desalting column to remove free dyes. FRET assays were carried out with 100 μl protein (5μM) on a Synergy H1 microplate reader (Bioteck) at room temperature. The excitation spectrum was scanned from wavelength 400 to 600 nm to determine the optimal excitation wavelength of labelled Alex 555 donor. The emission spectrum was recorded from wavelength 600 to 700 nm.

**Molecular dynamics simulation**— The crystal structure of YfkE from the protein data bank (PDB ID 4KJS) was used as the starting structure for the MD simulation. Missing residues at the loop regions were modeled using JACKAL (http://honig.c2b2.columbia.edu/jackal). To assign charges to the titratable residues at neutral pH, we used the pKa prediction algorithm PROPKA (http://nbcr-222.ucsd.edu/pdb2pqr_2.0.0/) and assigned charges to all titratable residues based on their standard protonation state at pH 7 except for H255, which was protonated. The protein was embedded in a planar bilayer made up of POPE and POPG lipids (3:1 molar ratio), which was generated using the Membrane Builder module of CHARMM-GUI (http://www.charmm-gui.org/). One leaflet of the bilayer, corresponding to the cytoplasmic side, contained 71 POPE and 31 POPG lipids while the other leaflet contained 70 POPE and 30 POPG lipids. The slight difference between the lipid numbers in the two monolayers accounts for the area difference between the two sides of the protein. The lipid-protein complex was placed in the center of a cubic box and solvated by TIP3P water molecules. 3 $Ca^{2+}$, 73 $Na^{+}$ and 12 $Cl^{-}$ ions were randomly placed in the water box to achieve a 140 mM ionic strength and simulate the system under the experimental [$Ca^{2+}$] condition. The system was energy-minimized and equilibrated with the lipid and protein heavy atoms harmonically restrained using a restraint of force constant of 4kcal/mol/$A^2$, which was progressively decreased to zero during a five-step equilibration run of 5ns total duration (time step = 1fs). A production run of 100 ns was then commenced with a constant number of particles (N), pressure (P = 1bar maintained by a Nose-Hoover Langevin piston), and temperature (T = 310K maintained by a Langevin thermostat) condition. Other simulation conditions include a periodic boundary condition, Particle Mesh Ewald (PME) electrostatic (5) with covalent bonds involving hydrogen atoms restrained by SHAKE, a 2fs time step, a switching function between 10 Å and 12 Å for non-bonded interactions, and a 14 Å cutoff for pair list updates. The simulation was conducted with the NAMD program (6) and the CHARMM36 force field (7). The same setup was used to conduct a control simulation in the absence of $Ca^{2+}$, increasing the number of $Na^{+}$ ions to 79 to maintain charge neutrality.

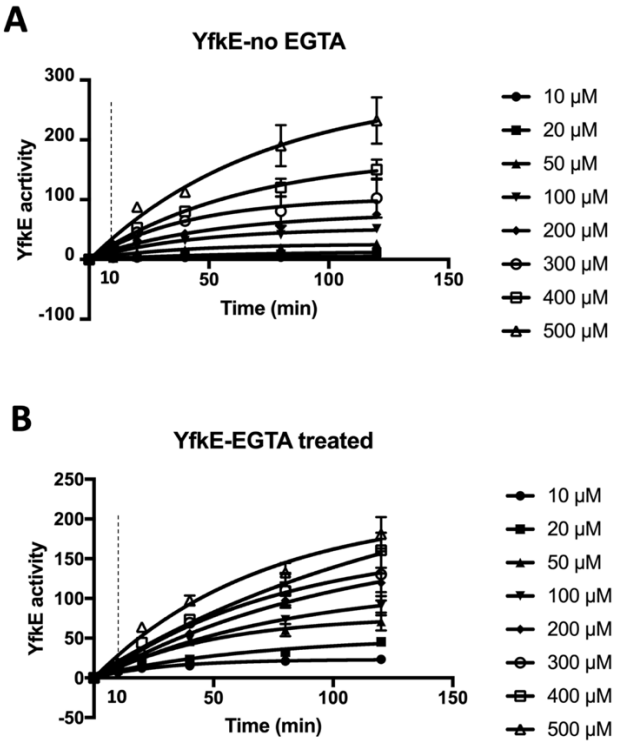


**Fig. S1. Time courses of Ca transport assays of YfkE$^{WT}$ measured using inside-out vesicles in the function of [$^{45}$Ca]$_{cyto}$. (A)** vesicles without EGTA treatment; **(B)** vesicles treated with 1mM EGTA. 10 min sampling time is marked with dashed lines. Data were fitted into single delay using the software Graphpad Prism 7. Error bars represent standard deviations of three independent experiments.

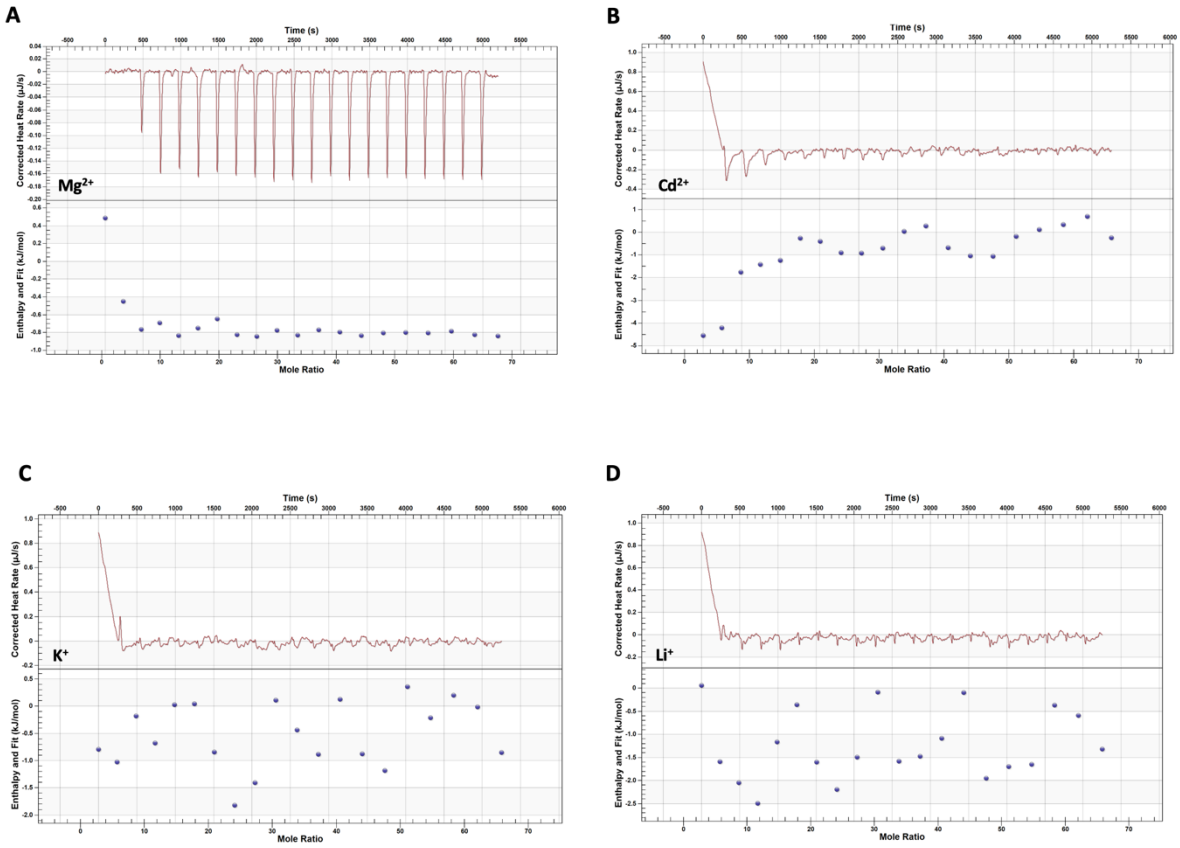


**Fig. S2. Cation interactions of the TM5-6 loop measured using isothermal titration calorimetry. (A)** $Mg^{2+}$; **(B)** $Cd^{2+}$; **(C)** $K^{+}$; and (**D**) $Li^{+}$. 2mM cation was titrated into 10 µM of a solution of the synthetic peptide representing the TM5-6 loop sequence of YfkE. Data analysis was carried out using the software NanoAnalyze.

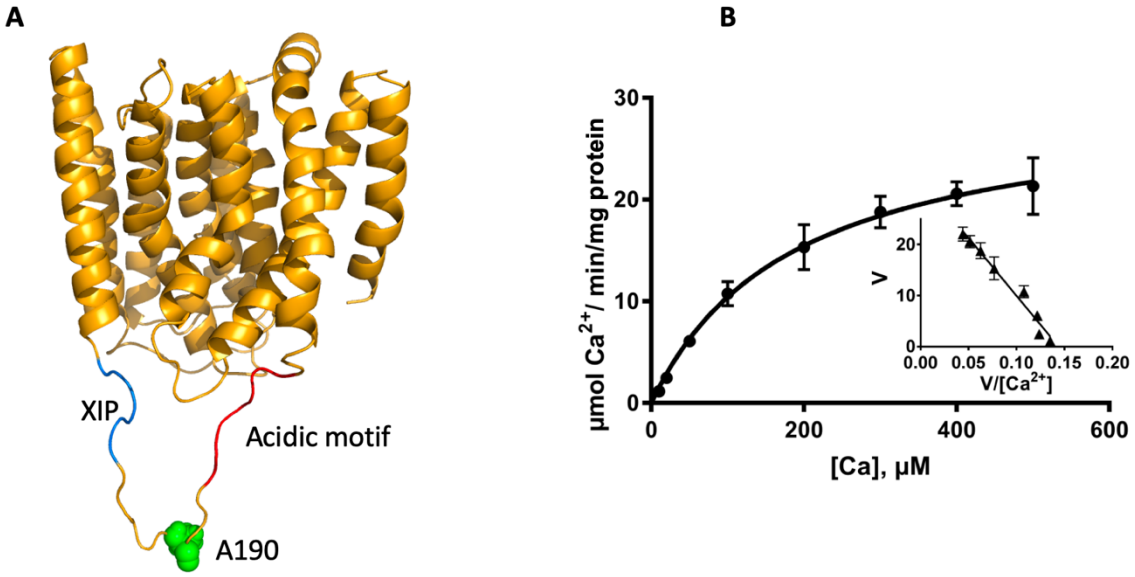


**Fig. S3. Fluorophore labeling of YfkE within the TM5-6 loop. (A)** Cartoon representation of the YfkE structure (*yellow*), showing the fluorophore labeling position at the A190 residue (*green* spheres) located between the XIP (*blue*) and acidic motif (*red*) regions within the TM5-6 loop. To demonstrate the position of the residue A190 within the TM5-6 loop, the structure of YfkE was shown using the rebuilt model for MD simulation (time=0). **(B)** $Ca^{2+}$ transport kinetics of the $YfkE^{A190C}$ mutant measured using ISO vesicles in the absence of EGTA. Data fitted into the Michaelis-Menten single exponential kinetics model yielded a $K_m$ of 186.7±13.4 μM and $V_{max}$ of 29.9±0.9 μmol/min/mg, which are similar to those of $YfkE^{WT}$. Eadie-Hofstee plot of the data showing mono-phasic kinetics is provided in the inner panel. Data analysis was carried out using the software GraphPad Prism 7. Error bars represent standard deviations of three independent experiments.

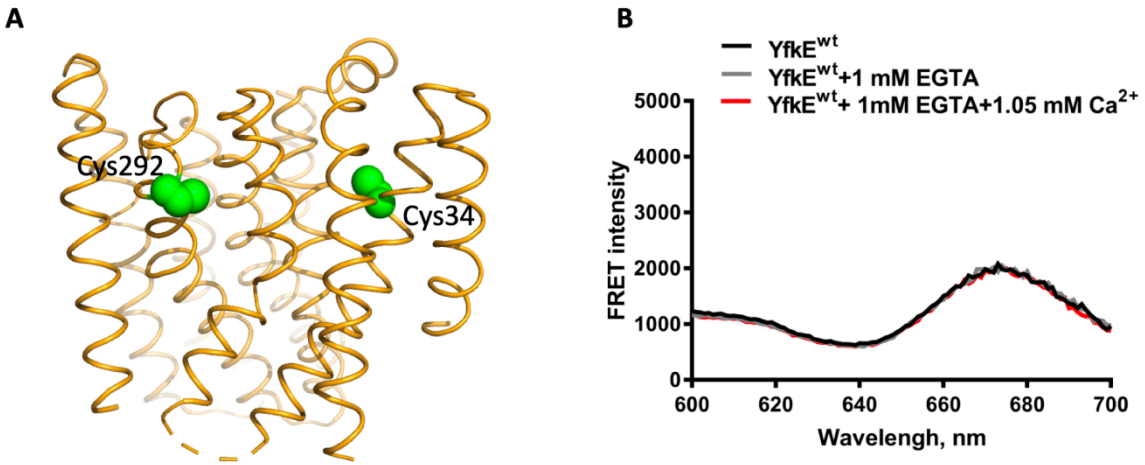


**Fig. S4. Endogenous cysteine residues in YfkE showing no effect on FRET measurements. (A)** Cartoon representation of YfkE (*yellow*), showing two endogenous cysteine residues, $Cys^{34}$ and $Cys^{292}$ (*green* spheres) embedded in the transmembrane helices. **(B)** Fluorescence spectra of $YfkE^{WT}$ protein, showing weak fluorescence signals and no changes in the presence or absence of $Ca^{2+}$. The protein was labeled with Alexa 555 and 647 maleimide using the same procedure described in the Materials and Methods section. Excitation wavelength is 555 nm.

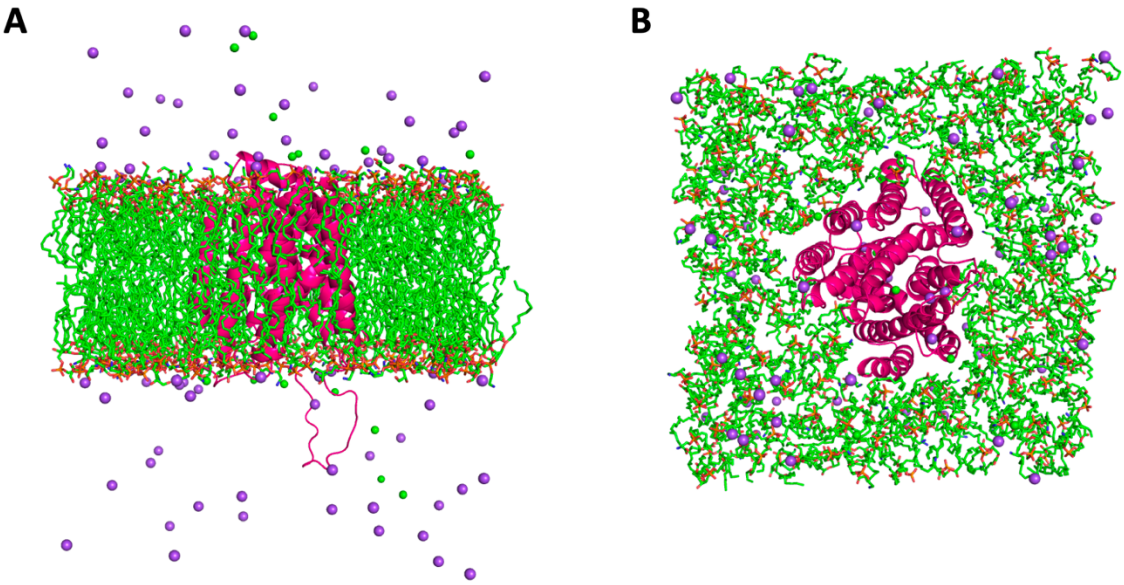


**Fig. S5. Setup of molecular dynamics simulation of YfkE in lipid bilayer. (A&B)** Cartoon representation of a snapshot at t = 0, showing a YfkE protomer (*magenta*) incorporated in a lipid bilayer consisting of POPE and POPG (70:30) (*red* and *green* sticks). $Na^+$ and $Cl^-$ ions are depicted as spheres in *purple* or *green*. Water molecules are removed for clarity. **(A)** View from the membrane bilayer; **(B)** view from the cytoplasmic side of the molecule.

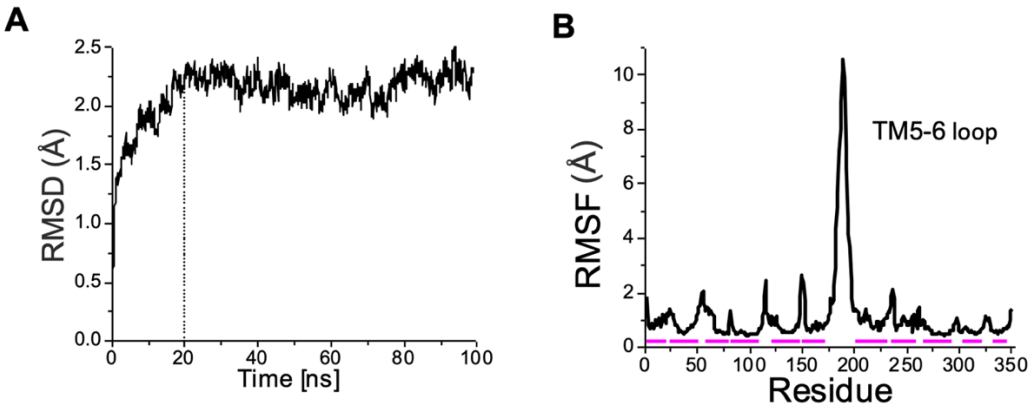


**Fig. S6. Conformational changes of YfkE in molecular dynamics simulation (+$Ca^{2+}$). (A)** Tome evolution of the TM helices backbone atom root mean square deviation (RMSD) from the equilibrated reference structure, indicating equilibration after about 20ns. **(B)** Root mean square fluctuations per residue (RMSF) showing the large conformational changes and dynamics at the TM5-6 loop region and to a lesser extent at the rest of the loops between TMs. The TM helices, indicated by *pink* bars, are very stable.

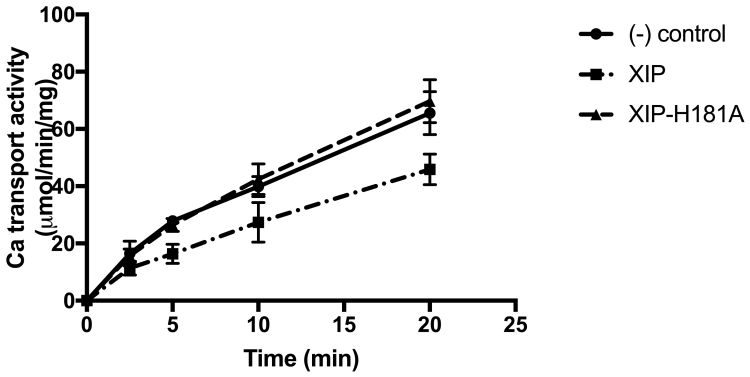


**Fig. S7**. **The role of the residue His$^{181}$ in XIP-mediated YfkE inhibition.** Time courses of $^{45}Ca^{2+}$ transport by YfkE$^{WT}$ in the presence of 5 μM synthetic peptide XIP-H181A (LVTARG), showing the loss of inhibition by the H181A mutation in contrast to the XIP wild type peptide (LVTHRG). Vesicles pre-treated with 1mM EGTA were used for assays. Error bars represent three independent experiments.

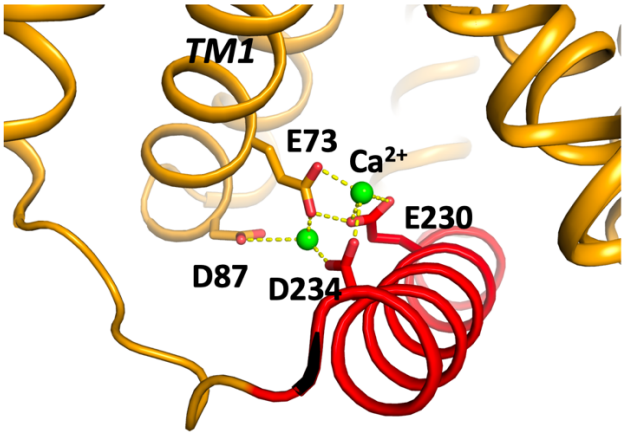


**Fig. S8. Regulatory $Ca^{2+}$ binding conformation of TM5-6 loop at the cytoplasmic entry of yeast VCX1.** The structure of VCX1 (8) from yeast is depicted as cartoon. Two $Ca^{2+}$ ions (*green* spheres) are coordinated by $Glu^{73}$ and $Asp^{87}$ (*yellow* sticks) from TM1 and $Glu^{230}$ and $Asp^{234}$ (*red* sticks) from the TM5-6 loop (*red* helix). The H-bond interactions with $Ca^{2+}$ are depicted as *yellow* dashed lines.

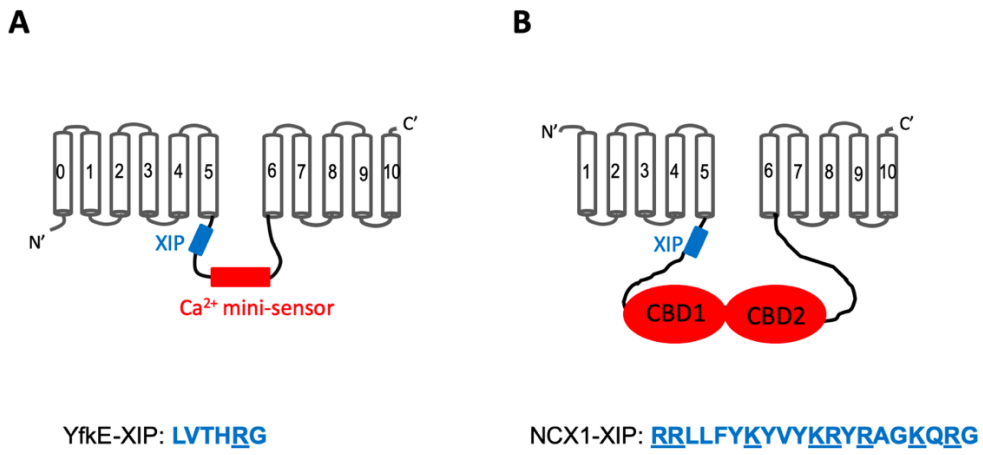


**Fig. S9. Conserved locations of XIP in prokaryotic YfkE and mammalian NCX1. (A)** Topological model of YfkE, showing XIP (*blue* bar) located adjacent to TM5 and followed by the $Ca^{2+}$ mini-sensor (*red* bar) within the TM5-6 loop. **(B)** Topological model of mammalian NCX1 showing XIP (*blue* bar) localized immediately after TM5 and at the upstream position of two regulatory $Ca^{2+}$ binding domains, CBD1 and CBD2 (*red* ovals). The XIP sequences of YfkE and mammalian NCX1 are provided, respectively. The two XIP segments share no sequence homology, but they both have an amphiphilic feature with positively charged residues underlined.

## Legends for Movies S1 to S2

**Movie S1 (separate file). Molecular dynamics simulation of YfkE in the presence of $Ca^{2+}$.** A YfkE protomer is depicted as *yellow* cartoon. Simulation time is 100 ns. A $Ca^{2+}$ ion (*green* sphere) was interacted with the acidic motif region (*red*) to induce allosteric conformational changes of the XIP fragment (*blue*) to move towards the $Ca^{2+}$ translation pathway. Lipids, water, and other ions in the simulation are removed for clarity.

**Movie S2 (separate file). Molecular dynamics simulation of YfkE in the absence of $Ca^{2+}$.** A YfkE protomer is depicted as *yellow* cartoon. Simulation time is 100 ns. The TM5-6 loop including the acidic motif region (*red*) and the XIP fragment (*blue*) remained random and disorder. Lipids, water, and other ions in the simulation are removed for clarity.

## SI references


1. Wu M*, et al.* (2013) Crystal structure of $Ca^{2+}/H^{+}$ antiporter protein YfkE reveals the mechanisms of $Ca^{2+}$ efflux and its pH regulation. *Proceedings of the National Academy of Sciences of the United States of America* 110(28):11367-11372.
2. Takahashi K (1977) The Reactions of Phenylglyoxal and Related Reagents with Amino Acids. *The Journal of Biochemistry* 81(2):395-402.
3. Studier FW (2005) Protein production by auto-induction in high density shaking cultures. *Protein expression and purification* 41(1):207-234.
4. Wu M, Wang M, Nix J, Hryshko LV, & Zheng L (2009) Crystal structure of CBD2 from the Drosophila $Na^{+}/Ca^{2+}$ exchanger: diversity of $Ca^{2+}$ regulation and its alternative splicing modification. *Journal of molecular biology* 387(1):104-112.
5. Darden TaY, Darrin and Pedersen, Lee (1993) Particle mesh Ewald: An N· log (N) method for Ewald sums in large systems. *The Journal of chemical physics* 98(12):10089--10092.
6. Phillips JC*, et al.* (2005) Scalable molecular dynamics with NAMD. *Journal of computational chemistry* 26(16):1781-1802.
7. Klauda JB, Monje V, Kim T, & Im W (2012) Improving the CHARMM force field for polyunsaturated fatty acid chains. *J Phys Chem B* 116(31):9424-9431.
8. Waight AB*, et al.* (2013) Structural basis for alternating access of a eukaryotic calcium/proton exchanger. *Nature* 499(7456):107-110.